Lead optimization of phthalazinone Phosphodiesterase inhibitors as novel antitrypanosomal compounds

*Irene G. Salado[a], Abhimanyu K. Singh[b#], Carlos Moreno-Cinos[a], Guna Sakaine[a,c], Marco Siderius[d], Pieter Van der Veken[a], An Matheeussen[e], Tiffany van der Meer[d], Payman Sadek[d], Sheraz Gul[f], Louis Maes[e], Geert-Jan Sterk[d], Rob Leurs[d], David Brown[b], Koen Augustyns[a]**

[a] Laboratory of Medicinal Chemistry, University of Antwerp, Universiteitsplein 1, B-2610 Antwerp, Belgium. [b] School of Biosciences, University of Kent, Canterbury, Kent, CT2 7NJ, United Kingdom. [c] Current address: Latvian Institute of Organic Synthesis, LV-1006 Riga, Latvia. [d] Medicinal Chemistry, Amsterdam Institute of Molecules, Medicines & Systems, Vrije Universiteit Amsterdam, Faculty of Science, 1081 Amsterdam, The Netherlands. [e] Laboratory for Microbiology, Parasitology and Hygiene (LMPH), University of Antwerp, Universiteitsplein 1, B-2610 Antwerp, Belgium.[f] Fraunhofer-IME SP, Schnackenburgallee 114, Hamburg, Germany.[#] Current address: Rega Institute for Medical Research, KU Leuven, 3000 Leuven, Belgium. *Corresponding author: Koen Augustyns, email address: koen.augustyns@uantwerpen.be

Table of contents:

Table S-1: Full antiparasitic screening panel and enzymatic activity on TbrPDEB1 and hPDE4 of the final compounds.

Comp.	*T.brucei*	*T.cruzi*	*L.infantum*	*P. falciparum*	MRC5	PMM	TbrPDEB1	hPDE4
1	6.35 ± 0.08	4.42 ± 0.05	4.19 ± 0.01	4.96 ± 0.23	4.35 ± 0.18	4.19 ± 0.01	7.36 ± 0.26	10.27 ± 0.17
2	6.45 ± 0.12	5.07 ± 0.03	5.20 ± 0.80	6.02 ± 0.48	4.93 ± 0.35	4.80 ± 0.50	7.18 ± 0.28	9.99 ± 0.18
3	5.77 ± 0.02	4.52 ± 0.01	4.48 ± 0.01	5.03 ± 0.18	4.75 ± 0.17	4.34 ± 0.21	6.98 ± 0.15	9.06 ± 0.22
4	6.06 ± 0.25	5.57 ± 0.10	5.36 ± 0.20	5.34 ± 0.23	5.13 ± 0.04	5.10 ± 0.01	6.19 ± 0.10	8.61 ± 0.05
5	5.75 ± 0.06	5.03 ± 0.01	4.77 ± 0.38	5.13 ± 0.31	4.19 ± 0.01	4.19 ± 0.01	6.47 ± 0.05	9.17 ± 0.08
6	5.77 ± 0.16	5.07 ± 0.02	4.69 ± 0.01	4.87 ± 0.11	4.19 ± 0.01	4.49 ± 0.01	6.19 ± 0.03	9.23 ± 0.24
7	6.58 ± 0.03	5.39 ± 0.51	4.69 ± 0.01	5.26 ± 0.23	5.52 ± 0.4	4.49 ± 0.01	6.19 ± 0.13	9.65 ± 0.21
8	5.44 ± 0.44	4.61 ± 0.59	4.85 ± 0.07	4.93 ± 0.15	5.41 ± 0.15	4.49 ± 0.01	6.59 ± 0.16	9.29 ± 0.06
9	5.73 ± 0.07	4.86 ± 0.36	4.63 ± 0.09	4.44 ± 0.12	4.76 ± 0.02	4.49 ± 0.01	6.96 ± 0.21	9.50 ± 0.21
10	5.64 ± 0.05	5.08 ± 0.03	4.37 ± 0.01	5.51 ± 0.27	4.19 ± 0.01	4.19 ± 0.01	6.16 ± 0.06	9.20 ± 0.26
11	6.44 ± 0.13	5.21 ± 0.22	4.91 ± 0.25	5.69 ± 0.48	4.22 ± 0.06	4.49 ± 0.01	7.37 ± 0.03	6.45 ± 0.11
12	6.09 ± 0.16	5.09 ± 0.04	5.18 ± 0.08	5.73 ± 0.06	5.11 ± 0.01	5.1 ± 0.01	7.61 ± 0.08	9.81 ± 0.05
14	5.73 ± 0.05	4.19 ± 0.00	4.19 ± 0.00	4.47 ± 0.00	4.19 ± 0.00	4.19 ± 0.00	7.68 ± 0.14	10.21 ± 0.08

15	5.74 ± 0.02	4.19 ± 0.01	4.19 ± 0.01	5.53 ± 0.04	4.19 ± 0.01	4.19 ± 0.01	7.12 ± 0.10	9.77 ± 0.04
16	4.19 ± 0.01	4.19 ± 0.01	4.19 ± 0.01	4.24 ± 0.01	4.19 ± 0.01	4.19 ± 0.01	7.01 ± 0.21	9.50 ± 0.14
17	6.32 ± 0.05	4.91 ± 0.12	4.49 ± 0.01	5.37 ± 0.32	4.50 ± 0.38	4.49 ± 0.01	7.51 ± 0.06	9.81 ± 0.03
24	5.7 ± 0.01	5.16 ± 0.2	5.40 ± 0.14	5.41 ± 0.36	4.19 ± 0.01	4.49 ± 0.01	6.08 ± 0.09	7.52 ± 0.16
25	5.68 ± 0.03	5.63 ± 0.03	5.45 ± 0.50	4.94 ± 0.29	4.19 ± 0.01	4.80 ± 0.43	<5.03	nd
26	5.72 ± 0.04	5.16 ± 0.07	5.64 ± 0.03	5.40 ± 0.24	4.19 ± 0.01	4.80 ± 0.43	<5.08	nd
27	4.88 ± 0.43	5.10 ± 0.77	4.93 ± 0.34	4.93 ± 0.36	4.42 ± 0.32	4.49 ± 0.01	<5.25	nd
28	4.19 ± 0.01	4.37 ± 0.25	4.49 ± 0.01	4.61 ± 0.05	4.53 ± 0.01	4.19 ± 0.01	7.11± 0.06	9.92 ± 0.23
29	4.99 ± 0.01	4.81 ± 0.46	4.99 ± 0.04	4.75 ± 0.06	4.19 ± 0.01	4.49 ± 0.01	<5.02	nd
30	4.49 ± 0.00	4.81 ± 0.48	4.79 ± 0.32	4.64 ± 0.08	4.39 ± 0.02	4.49 ± 0.01	<4.78	nd
31	4.48 ± 0.01	5.1 ± 0.01	4.79 ± 0.43		4.19 ± 0.01	4.19 ± 0.01	<5.34	nd
32	4.32 ± 0.18	4.70 ± 0.29	4.43 ± 0.09		4.51 ± 0.04	4.19 ± 0.01	<5,01	nd
35	6.00 ± 0.42	4.37 ± 0.02	4.34 ± 0.21	5.57 ± 0.05	4.19 ± 0.01	4.34 ± 0.21	6.39 ± 0.01	9.52 ± 0.14
36	5.12 ± 0.06	4.34 ± 0.2	4.24 ± 0.07	5.39 ± 0.39	4.19 ± 0.01	4.19 ± 0.01	6.11 ± 0.04	9.32 ± 0.08
37	5.30 ± 0.07	5.11 ± 0.01	5.09 ± 0.18	5.14 ± 0.14	4.61 ± 0.33	4.80 ± 0.43	6.05 ± 0.11	7.20 ± 0.15
38	5.17 ± 0.01	5.68 ± 0.02	5.09 ± 0.01	5.42 ± 0.04	4.19 ± 0.01	4.80 ± 0.43	<5.67	nd

39	5.48 ± 0.36	5.19 ± 0.04	5.08 ± 0.02	5.41 ± 0.07	4.19 ± 0.01	4.80 ± 0.43	<5.78	nd
41	4.19 ± 0.01	4.19 ± 0.01	4.19 ± 0.01	4.19 ± 0.01	4.19 ± 0.01	4.19 ± 0.01	<4.50	nd
42	4.49 ± 0.01	4.19 ± 0.01	4.27 ± 0.11	4.27 ± 0.11	4.19 ± 0.01	4.19 ± 0.01	<4.50	nd
43	4.19 ± 0.01	4.19 ± 0.01	4.19 ± 0.11	4.27 ± 0.01	4.19 ± 0.01	4.19 ± 0.01	<4.74	nd
44	6.06 ± 0.23	5.09 ± 0.02	5.03 ± 0.09	5.21 ± 0.56	4.37 ± 0.20	4.65 ± 0.30	7.03 ± 0.20	9.18 ± 0.16
45	5.71 ± 0.16	4.8 ± 0.36	4.52 ± 0.06	5.21 ± 0.51	4.90 ± 0.24	4.19 ± 0.01	<5.01	nd
46	4.34 ± 0.21	4.37 ± 0.24	4.56 ± 0.19		4.37 ± 0.24	4.19 ± 0.01	<4.65	nd
47	5.12 ± 0.01	5.09 ± 0.01	5.09 ± 0.01	5.13 ± 0.29	4.19 ± 0.01	4.19 ± 0.01	<5.16	nd
48	5.71 ± 0.01	4.39 ± 0.12	4.33 ± 0.19	5.11 ± 0.41	4.25 ± 0.07	4.19 ± 0.01	7.07 ± 0.18	9.79 ± 0.28
49	5.19 ± 0.03	5.00 ± 0.05	4.77 ± 0.29	5.31 ± 0.26	4.19 ± 0.01	4.42 ± 0.11	<5.80	nd
51	5.11 ± 0.11	4.9 ± 0.01	4.59 ± 0.14	5.17 ± 0.72	4.95 ± 0.06	4.49 ± 0.01	<5.43	nd
56	4.49 ± 0.01	4.96 ± 0.05	4.58 ± 0.08	5.54 ± 0.03	4.60 ± 0.02	4.49 ± 0.01	<5.69	nd
59	5.11 ± 0.03	4.77 ± 0.01	4.41 ± 0.07	5.73 ± 0.05	4.19 ± 0.01	4.29 ± 0.17	6.56 ± 0.01	8.93 ± 0.07
60	4.82 ± 0.39	4.19 ± 0.01	4.29 ± 0.17	6.13 ± 0.23	4.19 ± 0.01	4.29 ± 0.17	6.54 ± 0.03	9.25 ± 0.04
61	5.74 ± 0.01	4.19 ± 0.01	4.19 ± 0.01	4.58 ± 0.32	4.19 ± 0.01	4.19 ± 0.01	6.99 ± 0.22	9.41 ± 0.09
62	5.94 ± 0.31	4.31 ± 0.16	4.38 ± 0.12	5.05 ± 0.36	4.19 ± 0.01	4.19 ± 0.01	7.04 ± 0.18	9.07 ± 0.17

63	5.6 ± 0.03	4.24 ± 0.07	4.39 ± 0.14	4.59 ± 0.42	4.19 ± 0.01	4.19 ± 0.01	6.77 ± 0.19	9.71 ± 0.09

Antiprotozoal assays

Antiprotozoal assays

In vitro assays

The antiprotozoal assays were performed at the Laboratory of Microbiology, Parasitology and Hygiene (LMPH), Antwerp University, adopting the set of standard protocols.[1] Inhibitory concentrations 50% (IC_{50} values) were determined from five 4-fold dilutions starting from a maximum concentration of 64 μM.

Cytotoxicity assay

Human lung fibroblast MRC-5_{SV2} cells (Sigma Aldrich) were cultured in Earl's MEM, supplemented with 5% heat-inactivated fetal bovine serum (FBSi), 20 mM L-glutamine and 16.5 mM sodium bicarbonate. Assays were performed in 96-well microtiter plates, each well containing 1×10^4 cells. After incubation for 72 h in a humidified atmosphere (37°C, 5% CO_2) and addition of resazurin, cell viability was assessed fluorimetrically (λ_{ex} 550 nm, λ_{em} 590 nm). The results are expressed as % reduction in cell growth/ viability compared to untreated control wells and IC_{50} values were determined. Tamoxifen was included as reference drug.

Trypanosoma brucei brucei assay

The suramin-sensitive strain *Trypanosoma b. brucei* Squib 427 was maintained in HMI-9- medium, supplemented with 10% FBSi. Assays were performed in 96-well microtiter plates, each well containing 10 μL of the dilution of compound together with 190 μL of the parasite suspension (7×10^4 parasites/mL). After incubation in a humidified atmosphere (37°C, 5% CO_2) for 72 h, resazurin was added for another 24 h and parasite growth was assessed fluorimetrically (λ_{ex} = 550 nm, λ_{em} = 590 nm). The results are

[1] Cos P, Vlietinck AJ, Berghe DV, Maes L. Anti-infective potential of natural products: how to develop a stronger in vitro 'proof-of-concept'. *J Ethnopharmacol.* ***2006****;106(3):290-302*

expressed as % reduction in parasite growth/viability compared to control wells. Suramin was included as reference drug.

Trypanosoma cruzi assay

The nifurtimox-sensitive *Trypanosoma cruzi*, Tulahuen CL2, β-galactosidase strain was maintained in MRC-5_{SV2} cells in MEM medium, supplemented with 200 mM L-glutamine, 16.5 mM sodium bicarbonate and 5% FBSi. Assays were performed in 96-well microtiter plates, each well containing 10 µL of the compound dilution and 190 µL of MRC-5_{SV2} cell/parasite inoculum (2×10^4 cells/mL and 2×10^5 parasites/mL). After incubation for 168 h, parasite growth was compared to untreated-infected controls. Parasite burdens were assessed after adding 50 µL/well of a stock solution containing 15.2 mg CPRG (chlorophenolredβ-D-galactopyranoside) and 250 µL Nonidet in 100 ml PBS. The change in color was measured spectrophotometrically at 540 nm after 4 h at 37 °C. The results were expressed as % reduction in parasite burdens compared to control wells. Nifurtimox was included as reference drug.

Leishmania infantum assay

Leishmania infantum MHOM/MA (BE)/67 was maintained in the golden hamster and spleen-derived amastigotes were collected for infection. Primary peritoneal mouse macrophages (PMM) were used as host cells and collected 48 h after peritoneal stimulation with a 2% potato starch suspension. Assays were performed in 96-well microtiter plates, each well containing 10 µL of the dilution of compound together with 190 µL of macrophage/parasite inoculum (3×10^5 cells and 3×10^6 parasites/well in RPMI-1640 + 5% FBSi). After incubation for 120 h, total parasite burdens were microscopically assessed after Giemsa staining. The results are expressed as % reduction in parasite burden compared to untreated control wells. Miltefosine was included as reference drug.

Plasmodium falciparum assay

The chloroquine-resistant strain of *P. falciparum* (Pf-K1) was maintained in RPMI-1640 supplemented with 0.37 mM hypoxanthine, 25 mM HEPES buffer, 25 mM sodium bicarbonate and 10% human 0^+ serum together with 2–4% washed human 0^+ erythrocytes. All cultures and assays were conducted under a humidified atmosphere (37°C, 4% CO_2, 3% O_2 and 93% N_2). Assays were performed in 96-well microtiter plates, each well containing 10 µL of the compound dilutions together with 190 µL of parasite inoculum (1% parasitaemia, 2% hematocrit). After incubation for 72 h, the plates were frozen and stored at −20°C. Upon thawing, 20 µL of each well was transferred into another plate together with 100 µL Malstat® reagent and 20 µL of a 1/1 mixture of PES (phenazine methosulfate, 2 mg/mL) and NBT (Nitro Blue Tetrazolium Grade III, 0.1 mg/ml). The plates were kept in the dark for 2 h and change in color was measured spectrophotometrically at 655 nm. The results are expressed as % reduction in parasitaemia compared to control wells. Chloroquine was included as reference drug.

Enzymatic assay protocol on TBrPDEB1 and hPDE4.

All assays are performed using the Lonza PDELight™ HTS cAMP phosphodiesterase Kit:

http://bio.lonza.com/uploads/tx_mwaxmarketingmaterial/Lonza_BenchGuides_PDELight_HTS_cAMP_phosphodiesterase_Kit.pdf

The assay is performed in Corning non-binding, low volume 384 well plates (article number: CLS3824-50EA) and Stimulation Buffer (S.B.) (50mM Hepes, 100mM NaCl, 10mM MgCl, 0.5mM EDTA, 0.05mg/ml BSA, pH 7.5)

Generation of dose-response curves and pKi calculation:

Three independently generated dose-response curves are generated for each compound.

Results

Data are analysed using GraphPad Prism and the Ki is calculated (μM) using the Cheng-Prusoff equation:

$$\mathbf{Ki} = \mathbf{IC^{50}} \div \left(\frac{\mathbf{[S]}}{\mathbf{Km}} + \mathbf{1}\right)$$

And then:

$$\mathbf{pKi} = -\mathbf{1} \times \mathbf{Log10}\ (\mathbf{Ki} \div \mathbf{1000000})$$

Microsomal stability

Components of the assay

Male mouse and human liver microsomes were purchased from commercial sources (Corning) and stored at -80°C. NADPH generating system solutions A and B and UGT reaction mix solutions A and B were purchased from a commercial source (Corning) and kept at -20°C.

Microsomal stability assay

The microsomal stability assay was carried out based on the BD Biosciences Guidelines for Use (TF000017 Rev1.0) (Addendum 2) with minor adaptations. The metabolic stability of the compounds was studied through the CYP450 superfamily (Phase-I metabolism) by fortification with reduced nicotinamide adenine dinucleotide phosphate (NADPH) and through uridine glucuronosyl-transferase (UGT) enzymes (Phase-II metabolism) by fortification with uridine diphosphate glucuronic acid (UDPGA). For the CYP450 and other NADPH dependent enzymes, both compounds were incubated at 5 μM together with 0.5 mg/mL liver microsomes in potassium phosphate buffer in a reaction started by the addition of 1 mM NADPH and stopped at the above listed sampling times. At these time points, 20 μl was withdrawn from the reaction mixture and 80 μl cold

acetonitrile (ACN), containing the internal standard tolbutamide, was added to inactivate the enzymes and precipitate the protein. The mixture was vortexed for 30 sec and centrifuged at 4 °C for 5 min at 15,000 rpm. The supernatant was stored at -80 °C until analysis. For the UGT enzymes, both compounds were incubated at 5 μM together with 0.5 mg/mL liver microsomes in a reaction started by the addition of 2 mM UDPGA cofactor.

Bioanalytical method

The corresponding loss of parent compound was determined using liquid chromatography (UPLC) (Waters AquityTM) coupled with tandem quadrupole mass spectrometry (MS^2) (Waters XevoTM), equipped with an electrospray ionization (ESI) interface and operated in multiple reaction monitoring (MRM) mode. The optimal MS parameters and control of the chromatographic separation conditions were tuned in a preceding experiment

Results

Raw results of mouse and human microsomal stability are shown in Tables S-2 – S-4. Each value is the mean of at least two experiments.

Table S-2. Mouse microsomal stability.

Microsomal stability												
		% remaining parent compound										
Microsomes	Phase I/II	Time (min)	**1**	**2**	**11**	**14**	**17**	**26**	**28**	**29**	**31**	**diclofenac**
Mouse	CYP450-NADPH	0	100	100	100	100	100	100	100	100	100	100
		15	31 ± 3.6	5.7 ± 3.1	8.3 ± 2.4	69 ± 0.4	10 ± 0.6	60 ± 6.1	50 ± 11.6	7.3 ± 1.9	7.2 ± 2.0	87 ± 2.3
		30	6.7 ± 1.5	1.7 ± 1.1	3.1 ± 0.6	43 ± 4.5	3.7 ± 3.5	35 ± 2.2	23 ± 8.2	1.1 ± 0.3	2.1 ± 1.2	70 ± 5.5
		60	1.9 ± 1.3	1.3 ± 0.1	2.3 ± 1.8	21 ± 2.1	1 ± 0.2	17 ± 3.3	7.2 ± 2.6	0.6 ± 0.2	3 ± 2.1	48 ± 1.2
	UGT enzymes	0	100	100	100	100	100	100	100	100	100	100
		15	102 ± 3.3	106 ± 2.9	87 ± 1.8	96 ± 1.5	99 ± 6.2	100 ± 15.5	113 ± 20.8	103 ± 11.8	107 ± 5.3	41 ± 1
		30	93 ± 0.4	102 ± 11	71 ± 1	99 ± 2.9	92 ± 9.2	95 ± 11	97 ± 8.9	97 ± 10.6	99 ± 1.1	44 ± 8
		60	99 ± 9.7	97 ± 24.3	54 ± 6.3	101 ± 1.2	91 ± 2.1	104 ± 2.3	106 ± 41.1	95 ± 11.1	122 ± 4.8	34 ± 2

Table S-3. Mouse microsomal stability.

Microsomal stability											
		% remaining parent compound									
Microsomes	Phase I/II	Time (min)	**35**	**38**	**44**	**45**	**47**	**48**	**49**	**61**	**diclofenac**
Mouse	CYP450-NADPH	0	100	100	100	100	100	100	100	100	100
		15	8.8 ± 3.3	58 ± 9.1	19 ± 2.3	6.6 ± 1.7	8.5 ± 1.1	49 ± 3.2	19 ± 11.2	0.4 ± 0.01	87 ± 2.3
		30	1.8 ± 1.3	44.9 ± 20.2	6.9 ± 0.5	0.4 ± 0.0	3 ± 1.2	20 ± 2.1	5 ± 3.2	0.6 ± 0.9	70 ± 5.5
		60	0.4 ± 0.3	16.3 ± 9.5	4.4 ± 0.2	3.5 ± 4.7	2.6 ± 0.7	3.4 ± 0.4	1 ± 0.8	0.1 ± 0.2	48 ± 1.2
	UGT enzymes	0	100	100	100	100	100	100	100	100	100
		15	98 ± 8.6	96 ± 12.6	81 ± 8.7	105 ± 6.4	106 ± 6	102 ± 1.2	101 ± 6.5	106 ± 7.6	41 ± 1
		30	101 ± 3.2	120 ± 0.4	58 ± 6.5	101 ± 0.8	106 ± 4.3	95 ± 3.2	96 ± 11.7	101 ± 1.3	44 ± 8
		60	100 ± 7.8	115 ± 4.3	38 ± 4.2	100 ± 9.4	100 ± 10.5	95 ± 0.2	105 ± 10.5	104 ± 4.5	34 ± 2

Table S-4. Human microsomal stability.*This experiment was performed only once.

Microsomal stability									
		% remaining parent compound							
Microsomes	Phase I/II	Time (min)	**1**	**2**	**11**	**14**	**17**	**26**	**Diclofenac***
Human	CYP450-NADPH	0	100	100	100	100	100	100	100
		15	56.7 ± 5.3	4.5 ± 1.5	6.1 ± 1.3	96 ± 4.1	2.1 ± 0.4	41 ± 18.6	44
		30	21.8 ± 4.9	0.9 ± 0.1	2.6 ± 1.7	89 ± 12.5	0.1 ± 0.1	23 ± 8.4	16
		60	5 ± 1.8	0.4 ± 0.2	1 ± 0.7	80 ± 9.2	0.1 ± 0.0	15 ± 10.3	3.8
	UGT enzymes	0	100	100	100	100	100	100	100
		15	98 ± 1.1	101 ± 0.0	4.9 ± 0.2	98 ± 6.5	93 ± 5.4	82 ± 10.7	21
		30	107 ± 4.2	103 ± 2.7	3.5 ± 0.3	108 ± 2.6	99 ± 6	59 ± 19.6	17
		60	109 ± 7.7	105 ± 0.1	2.2 ± 0.3	100 ± 2.6	95 ± 0.3	55 ± 10.6	11

Microsomal stability									
		% remaining parent compound							
Microsomes	Phase I/II	Time (min)	**28**	**35**	**38**	**44**	**48**	**61**	**diclofenac**
Human	CYP450-NADPH	0	100	100	100	100	100	100	100
		15	73 ± 3	33 ± 0.4	63 ± 5.5	12 ± 1.1	58 ± 2.3	3.9 ± 0.4	44
		30	48 ± 3	11 ± 2.4	37 ± 6.7	4.2 ± 2.9	43 ± 4.1	0.3 ± 0.4	16
		60	23 ± 0.5	1.4 ± 0.8	14 ± 4.8	2.7 ± 2.2	23 ± 3.1	0.3 ± 0.1	3.8
	UGT enzymes	0	100	100	100	100	100	100	100
		15	120 ± 9.7	97 ± 0.4	114 ± 1.1	4.6 ± 0.9	104 ± 0.2	100 ± 5	21
		30	133 ± 3.4	98 ± 2.7	86 ± 1.9	4.2 ± 0.9	104 ± 4.3	105 ± 2.7	17
			136 ± 17.9	101 ± 2.8	112 ± 19.3	3.2 ± 0.5	102 ± 2	105 ± 1.3	11

Production of recombinant TbrPDEB1 and hPDE4D2 catalytic domains

A gene segment coding for TbrPDEB1 catalytic domain residues 565–918 (Uniprot entry Q8WQX9) was PCR amplified and cloned into *E. coli* expression vector pET28a(+) using *Nde*I and *EcoR*I restriction sites. The resulting vector was named pET28a(+)-TbrPDEB1_CD. Similarly, PCR amplification of the coding sequence for hPDE4D2 catalytic domain residues 381–740 (Uniprot entry Q08499) was performed and the product was cloned into a pET15b(+) *E. coli* expression vector using *Nde*I and *Xho*I restriction sites. The resulting vector was named pET15b(+)-hPDE4D_CD. Vector encoded N-terminal 6xHis tag was kept in frame for both constructs to facilitate purification.

For expression, TbrPDEB1_CD transformed *E. coli* BL21(DE3) cells were allowed to grow in 2xYT media at 37 °C until the optical density at 600 nm reached 0.6–0.8. The temperature was reduced by cooling and the cultures were induced with 1 mM isopropyl b-d-1-thiogalactopyranoside followed by overnight growth at 16 ^{O}C. Cells were collected by centrifugation, resuspended in lysis buffer (20 mM Tris-HCl pH 7.5, 200 mM NaCl, 10 mM imidazole, 5% glycerol, 2 mM β-mercaptoethanol (BME), protease inhibitor cocktail tablet) and lysis was performed using a cell disruptor (20 kpsi / 1 pass). Cleared cell lysate was loaded onto a 5 mL HisTrap HP nickel affinity column (GE Healthcare Biosciences) and bound protein was eluted with a linear gradient of 0–1 M imidazole. Pooled fractions were desalted to remove imidazole and the N-terminal 6xHis tag was

removed by overnight incubation at 4 °C with human thrombin (Abcam or Sigma-Aldrich). Any tagged fraction was removed by a second nickel affinity purification step and the protein was loaded onto a 5 ml HiTrap Q HP column (GE Healthcare Biosciences) prequilibrated with ion exchange buffer (20 mM Tris-HCl pH 7.5, 100 mM NaCl, 5% glycerol, 2 mM BME). Elution was performed with a linear gradient of 0–1 M NaCl and the pooled fractions were subjected to size exclusion chromatography step using a Superdex 200 increase 10/300 GL column (GE Healthcare Biosciences) prequilibrated in a buffer containing 20 mM Tris-HCl pH 7.5, 50 mM NaCl, 5% glycerol, 2 mM BME. The eluted protein was stored in the same buffer from which NaCl was removed prior to crystallization trials.

Expression and purification of hPDE4D2 catalytic domain was performed in a similar way as for TbrPDEB1-CD with the following changes in buffers used: cell lysis and nickel affinity chromatography buffer (50 mM Tris-HCl pH 8, 150 mM NaCl, 5 mM BME, 20 mM imidazole), ion exchange chromatography buffer (50 mM Tris-HCl pH 8, 50 mM NaCl, 5 mM DTT) and size exclusion chromatography buffer (50 mM Bis-tris pH 6.8, 100 mM NaCl, 5 mM DTT).

Crystallisation, diffraction data collection and structure solution of inhibitor complexes:

Crystals of TbrPDEB1-CD and hPDE4D2-CD were obtained in 24 well XRL plates (Molecular Dimensions) by vapor diffusion hanging drop technique, typically with 500 µL reservoir volume and 2 µL droplets with a protein to crystallization solution ratio of 1:1. Crystals of

TbrPDEB1-CD were obtained in a condition containing 20% PEG 3350, 400 mM sodium formate, 300 mM guanidine, 100 mM MES, pH 6.5 at 4 °C and that of hPDE4D2-CD in

24% PEG 3350, 30% ethylene glycol and 100 mM HEPES, pH 7.5 at 19 °C. For soaking experiments, 10-15 mM solutions of inhibitors NPD-226, NPD-356, NPD-1086 and NPD-1439 were prepared in respective crystal growth conditions and crystals were allowed to soak from overnight to 48 hours duration. In case of TbrPDEB1-CD, the soaked crystals were briefly dipped in soaking solutions supplemented with 15% glycerol for cryo protection, mounted on CryoLoop (Hampton Research) or LithoLoops (Molecular Dimensions) and vitrified in liquid nitrogen for data collection. Soaked hPDE4D2-CD crystals were harvested in a similar way, albeit without any cryo protection step. X-ray diffraction data sets were collected at Diamond Light Source (DLS; Didcot, Oxfordshire, UK) beamline I03 and processed by xia2[27] or autoPROC,[28] which incorporates XDS[29] and AIMLESS,[30] or were integrated using iMOSFLM[31] and reduced using POINTLESS, SCALA and TRUNCATE, all of which are part of CCP4.[32]

Structure solution, refinement and analysis

Structure of inhibitor bound complexes were determined by molecular replacement using CCP4 suite program Phaser[33] that utilised apo models of TbrPDEB1-CD (PDB id: 4I15) and hPDE4D2-CD (PDB id: 3SL3) as search templates or by direct Fourier synthesis method. Ligand descriptions were generated by ACEDRG available within the CCP4 pacakage[32]. Manual model adjustment and ligand fitting were performed in COOT[34] followed by model refinement with REFMAC.[35] Fully refined models were validated with MOLPROBITY.[36] Data collection and refinement statistics are given in Table 2S and 3S. Figures were prepared with PyMOL[37]. Coordinates of the structures have been deposited to the RCSB Protein Data Bank with following accession codes: 6FDS (TbrPDEB1–compound **1**); 6FDW (TbrPDEB1–compound **11**); 6FDX (TbrPDEB1–compound **12**); 6FE3 (TbrPDEB1–compound **35**); 6FDI (hPDE4D–compound **1**); 6FE7

(hPDE4D- compound **11**); 6FEB (hPDE4D– compound **12**); 6FET (hPDE4D– compound **12**).

Table S-5. Data collection and refinement statistics for TbrPDEB1 catalytic domain crystals in complex with various inhibitors

	1	**11**	**12**	**14**	**35**
Data collection					
Space group	*C* 1 2 1	*C* 1 2 1	*C* 1 2 1	*C* 1 2 1	*C* 1 2 1
Molecule/a.s.u	2	2	2	2	2
Cell dimensions					
a, *b*, *c* (Å)	112.72, 120.17, 68.17	111.69, 119.26, 67.97	114.10, 116.38, 68.31	116.20, 114.61, 68.38	115.53, 114.82, 68.31
α, β, γ (°)	90, 108.05, 90	90, 108.38, 90	90, 108.67, 90	90, 108.36, 90	90, 108.25, 90
Resolution (Å)	79.98-2.20	33.91-1.96 (2.01-1.96)	57.10-2.31 (2.35-2.31)	79.47-2.47 (2.52-2.47)	57.41-1.62 (1.66-1.62)

	(2.26-2.20) *				
R_{merge}	0.050	0.046	0.051	0.377	0.049
	(0.364)	(0.937)	(0.501)	(1.29)	(0.817)
$I / \sigma I$	10.1 (2.5)	13.6 (1.4)	12.3 (2.5)	4.4 (1.8)	11.6 (1.1)
CC(1/2)	0.998	0.999	0.999	0.916	0.998
	(0.902)	(0.604)	(0.910)	(0.366)	(0.593)
Completeness (%)	99.5 (99.7)	99.5 (99.8)	97.1 (96.7)	98.1 (98)	97.0 (80.4)
Redundancy	2.8 (2.9)	3.4 (3.4)	3.4 (3.5)	3.3 (3.4)	3.3 (2.5)
Refinement					
Resolution (Å)	2.20	1.96	2.31	2.47	1.62
No. reflections	41186	57112	34309	28048	98640
	(2964)	(4263)	(2518)	(2059)	(6027)
R_{work} / R_{free}	0.193/0.240	0.190/0.237	0.169/0.232	0.206/0.254	0.165/0.190
No. atoms					
Protein	5260	5252	5260	5260	5268
Ligand	80	74	76	74	44^
Water	178	232	144	373	500
B-factors					
Protein	63.67	53.16	67.39	23.27	32.20
Ligand	77	53.73	63.28	39.77	42.24
R.m.s. deviations					
Bond lengths (Å)	0.014	0.017	0.013	0.011	0.019
Bond angles (°)	1.612	1.796	1.607	1.442	1.817

PDB accession no.	6FDS	6FDW	6FDX	6FV9	6FE3
PDB ligand code	D5T	D62	D5Z	E8H	D68

Data were collected from one crystal in each case. *Values in parentheses are for highest-resolution shell. ^Ligand present at only one protein molecule

Table S-6. Data collection and refinement statistics for hPDE4D catalytic domain crystals in complex with various inhibitors

	1	**11**	**12**	**14**	**35**
Data collection					
Space group	$P\,2_1\,2_1\,2_1$	$P\,2_1\,2_1\,2_1$	$C\,2\,2\,2_1$	$P\,2_1\,2_1\,2_1$	$P\,2_1\,2_1\,2_1$
Molecule/a.s.u	4	4	2	4	4
Cell dimensions					
a, *b*, *c* (Å)	98.80, 111.04, 161.08	98.22, 111.03, 160.96	95.06, 158.23, 111.40	99.11, 110.71, 161.49	97.19, 110.71, 161.48
α, β, γ (°)	90, 90, 90	90, 90, 90	90, 90, 90	90, 90, 90	90, 90, 90
Resolution (Å)	67.10-1.90 (1.93-1.90) *	54.30-2.0 (2.05-2.0)	81.49-1.92 (1.96-1.92)	65.23-1.78 (1.83-1.78)	55.35-1.88 (1.93-1.88)
R_{merge}	0.105 (1.160)	0.100 (1.300)	0.061 (0.844)	0.061 (0.684)	0.085 (1.727)
$I / \sigma I$	11.8 (1.6)	12.3 (1.5)	19.3 (2.2)	15.0 (2.0)	13.7 (1.2)
CC(1/2)	0.996 (0.620)	0.999 (0.547)	0.999 (0.723)	0.999 (0.725)	0.999 (0.498)

Completeness (%)	100 (100)	100 (100)	99.1 (99.5)	100 (100)	100 (100)
Redundancy	6.8 (6.6)	6.7 (6.8)	6.6 (6.8)	6.4 (5.5)	6.7 (6.6)
Refinement					
Resolution (Å)	1.90	2.0	1.92	1.78	1.88
No. reflections	132610 (9723)	113139 (8333)	59752 (4401)	160321 (11606)	134495 (9815)
R_{work} / R_{free}	0.174/0.200	0.170/0.200	0.160/0.196	0.177/0.214	0.171/0.199
No. atoms					
Protein	10573	10532	5246	10531	10523
Ligand	160	148	114	148	176
Water	831	670	302	941	625
B-factors					
Protein	31.33	40.18	39.26	30.88	39.90
Ligand	35.08	48.18	45.58	36.88	45.02
R.m.s. deviations					
Bond lengths (Å)	0.014	0.018	0.014	0.019	0.018
Bond angles (°)	1.599	1.894	1.625	1.900	1.881
PDB accession no.	6FDI	6FE7	6FEB	6FW3	6FET
PDB ligand code	D5T	D62	D5Z	E8H	D68

Data were collected from one crystal in each case. *Values in parentheses are for highest-resolution shell. ^Ligand present at only one protein molecule

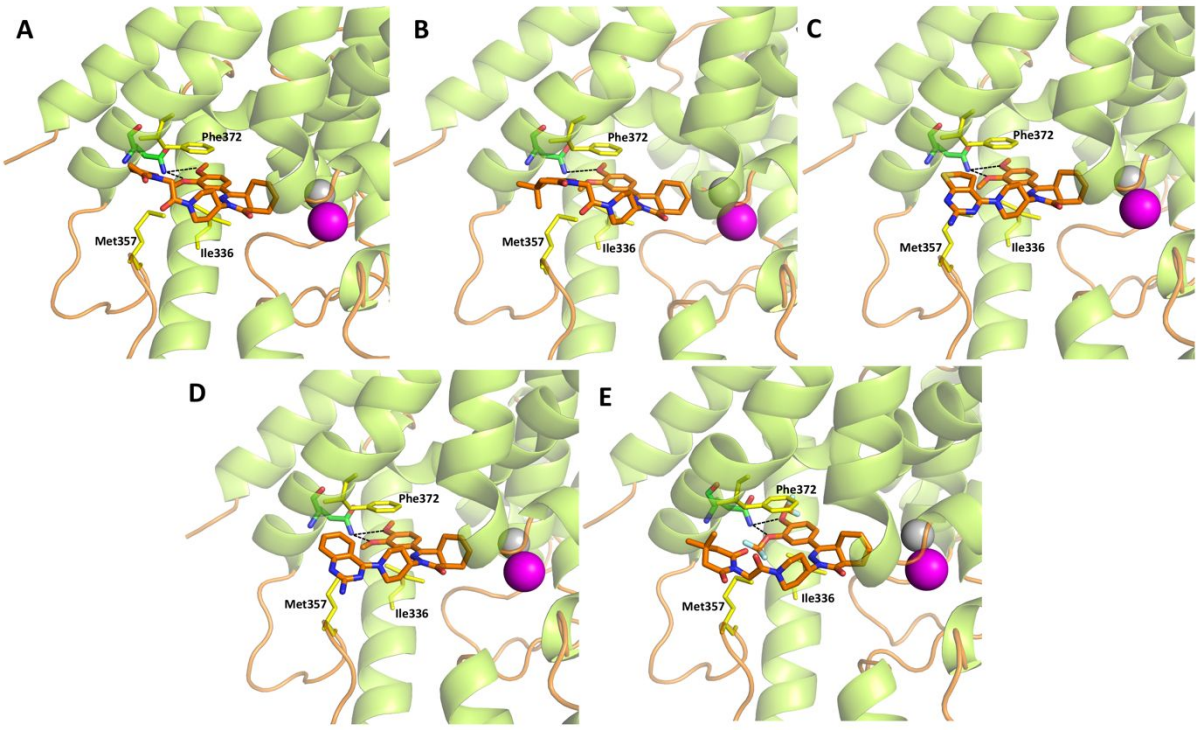

Figure S-1. Crystal structure of hPDE4D in complex with selected inhibitors: compound **14** (panel A), compound **1** (panel B), compound **11** (panel C), compound **12** (panel D) and compound **35** (panel E). Inhibitors are shown in orange sticks, metal center ions magnesium and zinc are shown in magenta and grey spheres respectively, residues Phe372 and Ile336, which forms the hydrophobic clamp, and Met357, which interacts with tail heterocyclics, are shown in yellow lines while conserved Gln369 is depicted by green sticks. Hydrogen bond interactions between Gln369 and phthalazinone substitutes are highlighted by black dashed lines.